

Malaphoric Z' models for $b \rightarrow s\ell^+\ell^-$ anomalies

Ben Allanach and Nico Gubernari

DAMTP, University of Cambridge, Wilberforce Road, Cambridge, CB3 0WA, United Kingdom

E-mail: ben.allanach.work@gmail.com, nico.gubernari@gmail.com

ABSTRACT: We study some phenomenological effects of kinetic mixing between the hypercharge field and a new $U(1)$ gauge field in specific Z' models that ameliorate the tensions between measurements and Standard Model predictions in $b \rightarrow s\ell^+\ell^-$ decays. To this end, we rederive the dimension-6 SMEFT coefficients resulting from integrating out the kinetically-mixed ('malaphoric') Z' field. The kinetic mixing provides a family-universal component to the couplings of the Z' field, which can improve fits to lepton flavour universality observables. We show how kinetic mixing improves the best fit of the $B_3 - L_2$ model to $b \rightarrow s$ data by 7.3 units of χ^2 while remaining compatible with other relevant data sets such as electroweak precision observables and measurements of $e^+e^- \rightarrow \ell^+\ell^-$ at LEP2.

KEYWORDS: B -anomalies, beyond the Standard Model, flavour changing neutral currents, SMEFT

Contents

1	Introduction	1
2	SMEFT Coefficients	4
3	$B_3 - L_2$ Model	7
4	Fits	9
5	Summary	13
A	WET Wilson Coefficients in the $B_3 - L_2$ model	15
B	Integrating out the X_μ field	15

1 Introduction

The B -meson decays mediated by a $b \rightarrow s\ell^+\ell^-$ transition are a powerful tool to test the validity of Standard Model (SM). In the last decades, the flavour physics community has invested substantial resources to improve the precision of both SM predictions and experimental measurements of these decays to obtain stronger constraints on physics beyond the SM (BSM). Whilst many such measurements are compatible with the SM [1, 2], those that are incompatible include the angular distribution and the branching ratio (BR) in $B \rightarrow K^* \mu^+ \mu^-$ decays [3–6], $BR(B \rightarrow K \mu^+ \mu^-)$ [7, 8], and $BR(B_s \rightarrow \phi \mu^+ \mu^-)$ [9]. These discrepant observables suffer from relatively large theoretical errors due to hard-to-calculate non-local QCD effects. Nevertheless, several estimates suggest that these effects are too small to resolve the discrepancies [10–13]. Two observables whose current measurements broadly agree [14] with SM predictions are R_K and R_{K^*} , where

$$R_M(q_{\min}^2, q_{\max}^2) := \frac{\int_{q_{\min}^2}^{q_{\max}^2} dq^2 \frac{dBR(B \rightarrow M \mu^+ \mu^-)}{dq^2}}{\int_{q_{\min}^2}^{q_{\max}^2} dq^2 \frac{dBR(B \rightarrow M e^+ e^-)}{dq^2}}, \quad (1.1)$$

for a meson M . This is important because, if one hypothesises BSM contributions to affect the aforementioned discrepant decays in observables involving di-muon pairs, the agreement of R_K and R_{K^*} with lepton flavour universality (LFU) may also imply some BSM effects in $b \rightarrow s e^+ e^-$ (plus CP -conjugate) decays.

set	quarks	EWPOs	LEP2	LFU	global
χ^2	419.	36.8	150.	18.5	624.
N	306	31	148	24	509
p	1.7×10^{-5}	.22	.44	.78	3.4×10^{-4}

Table 1. SM fit to `flavio2.6.1` data sets (shown as the middle four column headings) used in the present paper. χ^2 is the common chi-squared statistic, N is the number of observables in the set and p is the p -value (here, of the SM hypothesis with the `flavio2.6.1` estimate of observables and uncertainties).

We display a SM fit provided by¹ `smelli2.4.1` [16] and `flavio2.6.1` [17] to various categories of observables in Table 1. The categories are pre-defined in `flavio2.6.1` (we have omitted certain categories which are not relevant for our analysis) and are:

- ‘quarks’: this category includes many of the aforementioned discrepant observables in angular distributions of $B \rightarrow K^* \mu^+ \mu^-$ decays, as well as branching ratios of $B \rightarrow K^{(*)} \mu^+ \mu^-$ in various bins. It also contains other observables which agree with their SM prediction such as ΔM_s , a measure of the amount of $B_s - \bar{B}_s$ mixing. ΔM_s constrains Z' models that couple to $\bar{b}s$ and $b\bar{s}$ such as the model which we shall study.
- ‘LEP2’: this category constitutes differential cross-sections for $e^+ e^-$ collisions producing di-lepton pairs at the CERN LEP and LEP2 colliders. The calculation of the likelihood of these observables is described in Ref. [18] where it was made available in a form that was interfaced with `flavio` and `smelli`. We will use identical computer code for this incorporation in the present paper. Note that this is the only category not included in the original `flavio` code.
- ‘EWPOs’: this category consists of the electroweak precision observables *without* a family universality assumption. Thus, for example, $BR(Z \rightarrow \mu^+ \mu^-)$ is measured separately to $BR(Z \rightarrow e^+ e^-)$, even though the SM predicts them to be equal. This is appropriate for models which distinguish between different families, such as the ones we shall study.
- ‘LFU’: this contains various lepton flavour universality variables. Of particular interest are R_K and R_{K^*} from (1.1) because they used [19] to exhibit significant deviations with respect to SM predictions (according to analyses by the LHCb experiment), but do so no longer [14].

Table 1 shows that the SM quality-of-fit is poor. While the EWPOs, LEP2 and LFU measurements are all compatible with the SM, the observables in the quarks category as a whole are

¹In `smelli2.4.1` and `flavio2.6.1`, the Wilson coefficients are run, converted and matched by `wilson2.3.2` [15]. We had `smelli2.4.1` first recalculate the covariances in the theoretical uncertainties, a step which has now been done for the user in `smelli2.4.2`.

distinctively incompatible with it. Many observables within the quarks category *are* compatible with SM predictions: the p -value omitting these is of course lower than the one quoted, but we stick to the pre-defined categories in `flavio2.6.1` in order to evade accusations of a-posteriori bias. Many of the observables in the quarks category have large theoretical uncertainties in their predictions: these are taken into account with a generous error budget in `flavio`. We shall next describe some recent attempts to ameliorate the fit to the observables in the ‘quarks’ category, while simultaneously still fitting the other categories of observables reasonably well.

In Refs. [20–22], the hypothesis of a TeV-scale Z' with certain family-dependent couplings was investigated and fit to pertinent B -decay data. Such a Z' results from a hypothesised $U(1)_X$ gauge symmetry with family-dependent charges for the SM fermions (plus three right-handed neutrinos) which is spontaneously broken at the TeV scale. The fermion charge assignment here was $B_3 - L_2$, third-family baryon number minus second-family lepton number. Mixing between left-handed bottom and strange quark fields provides a coupling between the Z' field and $\bar{b}s + h.c.$, whereas the Z' field couples directly to di-muon pairs because the muon field’s $U(1)_X$ charge is non-zero. However, as described above, R_K and R_{K^*} became compatible with their SM predictions more recently than the original papers (i.e. Refs. [20–22]). Given the absence of a direct coupling between the Z' and di-electron pairs in the $B_3 - L_2$ model, the parameter space region that successfully explains the discrepant muon observables no longer adequately describes the updated experimental values of R_K and R_{K^*} [23]. While this region still represents a significant improvement over the SM, it is no longer able to reconcile both sets of measurements simultaneously.

To the best of our knowledge, Z' explanations of the $b \rightarrow s\ell^+\ell^-$ anomalies, including the $B_3 - L_2$ model, have all neglected kinetic mixing between the $U(1)_X$ gauge boson field and the hypercharge gauge boson field. Such a mixing term in the Lagrangian density is gauge invariant and thus allowed. Even if it is not present, it will be generically induced by loop effects. However, if one has a reason to suppose that the mixing effects are zero at a certain larger scale (for example because $SU(3) \times SU(2) \times U(1)_Y \times U(1)_X$ becomes embedded in some appropriate semi-simple group at that scale), then loop corrections will be small and neglecting the kinetic mixing term should be a good approximation.

In the present paper we shall, for the first time, explore the possibility that the kinetic mixing term is sizeable, dubbing the resulting models ‘malaphoric Z' models’. The kinetic mixing will introduce a family universal component to the couplings of the Z' field to leptons (as well as to other fermionic fields), and this can improve the fit to R_K and R_{K^*} whilst still fitting the other discrepant flavour data². We shall take the example of the $B_3 - L_2$ model and add the effects of sizeable kinetic mixing in order to examine quantitatively how the fit to measurements changes.

²Mixing with the hypercharge boson will affect the EWPOs, and the Z' -di-electron coupling will affect the LEP2 data. Thus, one can understand why the four categories of observables in Table 1 are important for our analysis.

In order to calculate such a change, we must inform `smelli2.4.1` and `flavio2.6.1` of the BSM effects in the form of SM effective field theory (SMEFT) dimension-6 coefficients, resulting from integrating out the Z' from the effective field theory. We shall present this calculation in §2, for generic fermionic charges. The fits to the $B_3 - L_2$ model, which we review in §3, will be presented in §4, both including the effects of kinetic mixing and neglecting it, for the purposes of illustration. We shall summarise and conclude in §5.

2 SMEFT Coefficients

The SMEFT coefficients of generic Z' models including the effects of kinetic mixing were recently calculated for the first time in Ref. [24]. We shall re-derive the dimension-6 coefficients, providing an independent check. As in Ref. [24], we start with a Lagrangian that contains the additional $U(1)_X$ gauge field³ X^μ and the hypercharge gauge boson field B^μ :

$$\mathcal{L}_{XB} = -\frac{1}{4}X_{\mu\nu}X^{\mu\nu} + \frac{1}{2}M_X^2X_\mu X^\mu - \frac{\epsilon}{2}B_{\mu\nu}X^{\mu\nu} - X_\mu J^\mu - B_\mu j^\mu. \quad (2.1)$$

Here, the $U(1)$ field strengths are defined as $X_{\mu\nu} := \partial_\mu X_\nu - \partial_\nu X_\mu$ and $B_{\mu\nu} := \partial_\mu B_\nu - \partial_\nu B_\mu$. The term proportional to ϵ in (2.1) is the one responsible for the kinetic mixing and $|\epsilon| \leq 1$ in order for the kinetic terms of both neutral gauge boson eigenstates to have the correct sign [25, 26]. The $U(1)_X$ -current is

$$J^\mu = g_X \sum_{\psi'} X_{\psi'} \bar{\psi}' \gamma^\mu \psi', \quad (2.2)$$

where $X_{\psi'}$ is the charge under $U(1)_X$ of the chiral fermionic field weak eigenstate ψ' , and g_X is the $U(1)_X$ gauge coupling. Note that in contrast to Ref. [24], we set X_H — the Higgs charge under $U(1)_X$ — to zero. This simplifies (2.2) and will be further motivated later. The sum in (2.2) and in the equation below runs over all chiral fermionic fields ψ' in the SM gauge group, i.e. q'_i, l'_i, e'_i, d'_i and u'_i . The hypercharge current is

$$j_\mu = ig'Y_H \left[H^\dagger D_\mu H - (D_\mu H)^\dagger H \right] + g' \sum_{\psi'} Y_{\psi'} \bar{\psi}' \gamma_\mu \psi'. \quad (2.3)$$

Here Y_H is the hypercharge of the Higgs field, Y_{ψ} is the hypercharge of the fermionic field ψ' and g' is the hypercharge gauge coupling. The electroweak covariant derivative is defined as

$$D_\mu = \partial_\mu + ig'Y_H B_\mu + igW_\mu^a T^a, \quad (2.4)$$

where g is the SM $SU(2)$ gauge coupling, W_μ^a are three $SU(2)$ gauge fields and T^a are the three generators of $SU(2)$ in the fundamental representation. Our conventions for $U(1)$ charges along with the other quantum numbers of the fields are tabulated in Table 2.

³In our discussions, we shall discriminate between the X^μ field, which is the (potentially) kinetically mixed gauge eigenstate spin-1 vector boson, versus the propagating eigenstate Z' .

Field ϕ	q'_i	l'_i	e'_i	d'_i	u'_i	H
$SU(3)$	3	1	1	3	3	1
$SU(2)$	2	2	1	1	1	2
Y_ϕ	1/6	-1/2	-1	-1/3	2/3	1/2
X_ϕ	X_{q_i}	X_{l_i}	X_{e_i}	X_{d_i}	X_{u_i}	0

Table 2. Representation of gauge eigenstates of matter and Higgs fields under $SU(3) \times SU(2) \times U(1)_Y \times U(1)_X$. The right-handed neutrino fields are assumed to be super-heavy and thus to play a negligible role in the collider phenomenology investigated here.

In order to calculate SMEFT coefficients, we integrate out the heavy field X_μ yielding (up to yet higher dimension operators) the dimension-6 Lagrangian density terms

$$\mathcal{L}_6 = -\frac{1}{2M_X^2} J_\mu J^\mu - \frac{\epsilon}{M_X^2} (\partial_\nu B^{\mu\nu}) J_\mu - \frac{\epsilon^2}{2M_X^2} (\partial_\nu B^{\mu\nu}) (\partial^\rho B_{\mu\rho}). \quad (2.5)$$

The procedure to integrate out the X_μ field is standard and is reported in Appendix B. Applying the 4-dimensional equation of motion (again, equivalently neglecting yet higher dimension operators) $j^\mu = -\partial_\nu B^{\mu\nu}$ to (2.5), we obtain the dimension-6 terms

$$\mathcal{L}_6 = -\frac{1}{2M_X^2} (J_\mu - \epsilon j_\mu) (J^\mu - \epsilon j^\mu), \quad (2.6)$$

which implicitly encodes the various SMEFT operators and coefficients. In order to extract the SMEFT coefficients in the down-aligned Warsaw basis [27] we expand (2.6) into the unprimed fermion mass eigenstates, for example

$$q'_i = (V_{d_L})_{ij} q_j. \quad (2.7)$$

In the *down-aligned* Warsaw basis, the q'_i fields are assumed to have already been rotated in family space: $q'_i = (V_q)_{ij} \tilde{q}_j$ from an initial field basis \tilde{q}_j such that $q'_i = (V_{ik} u'_{L_k}, d'_{L_i})$, where $(V_q)_{ij}$ are elements of some unitary 3 by 3 matrix and V is the CKM matrix [28]. The mass eigenstates of the u_i, d_i, e_i fields are assumed to coincide with those of the concomitant gauge eigenstates, i.e. $u_i = u'_i, d_i = d'_{L_i}, e_i = e'_{L_i}$. e_{L_i} is also assumed to coincide with e'_{L_i} whereas V_{d_L} necessarily will contain some family mixing (in order to facilitate certain $b \rightarrow s$ transitions), to be defined in more detail below.

Expanding (2.6) in terms of the fields leads to the calculation of the SMEFT Wilson coefficients in the down-aligned Warsaw basis [27]. The dimension-6 SMEFT coefficients we present are initially in a *redundant* basis, where the family indices i, j, k and l take values $\in \{1, 2, 3\}$ and for example both C_{ll}^{iiji} and C_{ll}^{jjii} are non-zero⁴, even though they must be equal. In our numerics, these are carefully converted to the *non-redundant* basis defined in Ref. [29] used in the Wilson Coefficient Exchange Format (WCXF) [30]. We shall explain

⁴From now on, repeated indices are left unsummed unless the summation is explicit.

(following each set of coefficients) how the expressions change in conversion to the WCXF format, if at all. We shall list only the *non-zero* dimension-6 SMEFT coefficients, starting with the 4-fermion operators in their mass eigenbasis

$$C_{ll}^{iijj} = -\frac{1}{2M_X^2} (g_X X_{l_i} - g' \epsilon Y_l) (g_X X_{l_j} - g' \epsilon Y_l), \quad (2.8)$$

$$C_{ee}^{iijj} = -\frac{1}{2M_X^2} (g_X X_{e_i} - g' \epsilon Y_e) (g_X X_{e_j} - g' \epsilon Y_e), \quad (2.9)$$

$$C_{uu}^{iijj} = -\frac{1}{2M_X^2} (g_X X_{u_i} - g' \epsilon Y_u) (g_X X_{u_j} - g' \epsilon Y_u), \quad (2.10)$$

$$C_{dd}^{iijj} = -\frac{1}{2M_X^2} (g_X X_{d_i} - g' \epsilon Y_d) (g_X X_{d_j} - g' \epsilon Y_d). \quad (2.11)$$

To convert to the WCXF non-redundant basis, one requires $j \geq i$ and multiplies each of the right-hand sides of (2.8)-(2.11) by a factor $(2 - \delta_{ij})$. In order to write down $C_{qq}^{(1)}$ in a succinct form, we first define

$$\Xi_{ij} := -Y_q g' \epsilon \delta_{ij} + g_X \sum_k (V_{d_L}^\dagger)_{ik} X_{q_k} (V_{d_L})_{kj}, \quad (2.12)$$

so that

$$(C_{qq}^{(1)})^{ijkl} = -\frac{1}{2M_X^2} \Xi_{ij} \Xi_{kl}. \quad (2.13)$$

Here, for this one set of SMEFT Wilson coefficients, converting to WCXF format is slightly more involved. We cycle through all possible values of $\{i, j, k, l\} \in \{1, 2, 3\}$, adding (2.13) (if it is equivalent) to the relevant coefficient of the 27 non-redundant $(C_{qq}^{(1)})^{ijkl}$ defined in Ref. [30]⁵. This automatically reproduces symmetry factors from the summands. We also have the non-identical 4-fermion operators (leaving the prime in $X_{\psi'}$ implicit for brevity's sake)

$$C_{le}^{iijj} = -\frac{1}{M_X^2} (g_X X_{l_i} - g' \epsilon Y_l) (g_X X_{e_j} - g' \epsilon Y_e), \quad (2.14)$$

$$C_{lu}^{iijj} = -\frac{1}{M_X^2} (g_X X_{l_i} - g' \epsilon Y_l) (g_X X_{u_j} - g' \epsilon Y_u), \quad (2.15)$$

$$C_{ld}^{iijj} = -\frac{1}{M_X^2} (g_X X_{l_i} - g' \epsilon Y_l) (g_X X_{d_j} - g' \epsilon Y_d), \quad (2.16)$$

$$C_{eu}^{iijj} = -\frac{1}{M_X^2} (g_X X_{e_i} - g' \epsilon Y_e) (g_X X_{u_j} - g' \epsilon Y_u), \quad (2.17)$$

$$C_{ed}^{iijj} = -\frac{1}{M_X^2} (g_X X_{e_i} - g' \epsilon Y_e) (g_X X_{d_j} - g' \epsilon Y_d), \quad (2.18)$$

$$(C_{ud}^{(1)})^{iijj} = -\frac{1}{M_X^2} (g_X X_{u_i} - g' \epsilon Y_u) (g_X X_{d_j} - g' \epsilon Y_d), \quad (2.19)$$

⁵For details, see the main program `kinetic_mixing.py` provided in the ancillary directory of the `arxiv` version of this paper.

which are already in the WCXF format. We also have the coefficients of 4-fermion operators involving only a single bilinear of the q_i fields

$$(C_{lq}^{(1)})^{iijk} = -\frac{1}{M_X^2} (g_X X_{l_i} - g' \epsilon Y_l) \Xi_{jk}, \quad (2.20)$$

$$C_{qe}^{iijk} = -\frac{1}{M_X^2} \Xi_{ij} (g_X X_{e_k} - g' \epsilon Y_e), \quad (2.21)$$

$$(C_{qu}^{(1)})^{iijk} = -\frac{1}{M_X^2} \Xi_{ij} (g_X X_{u_k} - g' \epsilon Y_u), \quad (2.22)$$

$$(C_{qd}^{(1)})^{iijk} = -\frac{1}{M_X^2} \Xi_{ij} (g_X X_{d_k} - g' \epsilon Y_d), \quad (2.23)$$

where, to convert to the WCXF, one requires $j \geq i$ and for $i \neq j$, Ξ_{ij} is replaced by $\Xi_{ij} + \Xi_{ji}^*$ in (2.20)-(2.23). The same conversion applies to

$$(C_{\varphi q}^{(1)})_{ij} = \frac{1}{M_X^2} g' \epsilon Y_H \Xi_{ij}. \quad (2.24)$$

No conversion is necessary to obtain the remaining non-zero coefficients in the WCXF:

$$(C_{\varphi l}^{(1)})^{ii} = \frac{1}{M_X^2} g' \epsilon Y_H (g_X X_{l_i} - g' \epsilon Y_l), \quad (2.25)$$

$$C_{\varphi e}^{ii} = \frac{1}{M_X^2} g' \epsilon Y_H (g_X X_{e_i} - g' \epsilon Y_e), \quad (2.26)$$

$$C_{\varphi d}^{ii} = \frac{1}{M_X^2} g' \epsilon Y_H (g_X X_{d_i} - g' \epsilon Y_d), \quad (2.27)$$

$$C_{\varphi u}^{ii} = \frac{1}{M_X^2} g' \epsilon Y_H (g_X X_{u_i} - g' \epsilon Y_u), \quad (2.28)$$

$$C_{\varphi \square} = -\frac{1}{2M_X^2} (\epsilon g' Y_H)^2, \quad (2.29)$$

$$C_{\varphi D} = -\frac{2}{M_X^2} (\epsilon g' Y_H)^2. \quad (2.30)$$

This completes the list of dimension-6 non-zero SMEFT Wilson coefficients resulting from integrating out the X^μ field. We shall now introduce a particular model for studying the effects of kinetic mixing.

3 $B_3 - L_2$ Model

We now briefly introduce the $B_3 - L_2$ model [20–22]. This model was devised so that the effects of the TeV-scale Z' field could explain the $b \rightarrow s\ell^+\ell^-$ anomalies. The $X := B_3 - L_2$ $U(1)_X$ charge assignments are displayed in Table 3. We had already set $X_H = 0$ because of the need to be able to write down a top Yukawa coupling in the model. Such a Yukawa coupling, being of order one, should be allowed in the set of renormalisable dimension-4 Lagrangian terms. The $U(1)_X$ symmetry is spontaneously broken by the flavon θ , which is assumed to

Field ϕ	q'_i	l'_i	e'_i	d'_i	u'_i	ν_i	H	θ
X_ϕ	δ_{i3}	$-3\delta_{i2}$	$-3\delta_{i2}$	δ_{i3}	δ_{i3}	$-3\delta_{i2}$	0	+1

Table 3. X charge assignments of fields in the $B_3 - L_2$ model. The flavon θ is a SM-singlet complex scalar field which is assumed to acquire a TeV-scale vacuum expectation value.



Figure 1. Feynman diagrams of the leading BSM contribution in the $B_3 - L_2$ model to: $b \rightarrow s\ell^+\ell^-$ observables (left), $B_s - \bar{B}_s$ mixing (right).

acquire a TeV-scale vacuum expectation value $\langle \theta \rangle$, resulting in a massive spin-1 bosonic field X^μ with Lagrangian mass parameter

$$M_X = g_X \langle \theta \rangle. \quad (3.1)$$

The model explains why $|V_{td}|$, $|V_{ts}|$, $|V_{ub}|$ and $|V_{cb}|$ are all small compared to unity: they are zero in the unbroken $U(1)_X$ limit but the limit receives small corrections from the spontaneous breaking of the gauge symmetry. In a similar vein, the model postdicts a suppression in flavour changing effects between the first two families of charged lepton. Searches for $\mu \rightarrow e\gamma$ confirm that the process is much suppressed, since an upper bound on the branching ratio of smaller than 10^{-12} has been placed [31].

The dimension-6 SMEFT coefficients resulting from integrating the Z' of the $B_3 - L_2$ model were calculated in Ref. [23] in the $\epsilon = 0$ limit. We have checked that these coefficients agree with the expressions presented in §2 in that limit.

The left-handed down quark mixing matrix is assumed to have the form

$$V_{d_L} = \begin{pmatrix} 1 & 0 & 0 \\ 0 & \cos \theta_{sb} & \sin \theta_{sb} \\ 0 & -\sin \theta_{sb} & \cos \theta_{sb} \end{pmatrix}. \quad (3.2)$$

In order to predict non-SM $b \rightarrow s$ mixing effects and explain some of the $b \rightarrow s\ell^+\ell^-$ anomalies as depicted in the left-hand panel of Fig. 1, one requires that $\theta_{sb} \neq 0$. This adds a tree-level flavour changing neutral current mediated by X_μ . $U(1)_X$ explanations of $b \rightarrow s\ell^+\ell^-$ anomalies such as the $B_3 - L_2$ model induce a BSM contribution to $B_s - \bar{B}_s$ mixing, as shown in the right-hand panel of the same figure. $B_s - \bar{B}_s$ mixing effects broadly agree with SM predictions and it is important that the measurable observable relevant to this (ΔM_s) is included in any flavour fits or constraints upon the model. `flavio2.6.1` computes the observable and it is included the observable in our fits in the ‘quarks’ category. We now go on to describe these fits and present the result of them.

$\hat{\epsilon}$	\hat{g}_X	θ_{sb}	$\Delta\chi^2_{\text{quarks}}$	$\Delta\chi^2_{\text{EWPO}}$	$\Delta\chi^2_{\text{LEP2}}$	$\Delta\chi^2_{\text{LFU}}$	$\Delta\chi^2_{\text{global}}$
0	0.082	-0.11	36.2	0.0	0.00	-3.8	32.8
-0.86	0.048	-0.19	40.1	-0.4	-0.02	0.8	40.1

Table 4. Fit to the $B_3 - L_2$ model [20–22] excluding (top line) and including (bottom line) sizeable kinetic mixing. p indicates the p –value of the best-fit point. $\Delta\chi^2 := \chi^2_{\text{SM}} - \chi^2$ in each category, so a higher value indicates a better fit. Input parameters are shown in the first three columns for $M_X = 3$ TeV.

4 Fits

The SMEFT coefficients are functions of the four BSM parameters: M_X , ϵ , g_X and θ_{sb} . However, notice that the SMEFT coefficients (2.8)–(2.30) only depend upon three free input BSM-parameter *combinations*, which can be chosen to be

$$\hat{\epsilon} := \epsilon(3 \text{ TeV})/M_X, \quad \hat{g}_X := g_X(3 \text{ TeV})/M_X, \quad \theta_{sb}. \quad (4.1)$$

One typically wishes to fix the renormalisation scale μ of the Wilson coefficients' boundary condition to be M_X itself in order to render unaccounted-for loop corrections small, since they are expected to be proportional to powers of $\log(M_X/\mu)$. The renormalisation down to the weak scale M_Z then brings in a separate dependence upon M_X , although such effects are small, being suppressed by a factor of order $\log(M_X/M_Z)/(16\pi^2)$. Since M_X is around the few-TeV scale, it is a good approximation (at the couple of percent level in relative change to Wilson coefficients) to neglect the additional M_X dependence. We shall present results for one particular representative value of $M_X = 3$ TeV but the approximate scaling is implicit because we use the variables $\hat{\epsilon}$ and \hat{g}_X defined in (4.1).

It was shown by Ref. [23] that the $\hat{\epsilon} = 0$ $B_3 - L_2$ model's fit to flavour data became less favourable with LHCb's reanalysis [14] of R_K and R_{K^*} (although it was still more favourable than the SM). One of the points of our present paper is that kinetic mixing introduces a Z' -di-electron vertex and can improve the fit. Therefore, we show the fits for the $B_3 - L_2$ mixing with and without including kinetic mixing (i.e. $\hat{\epsilon} = 0$ and $\hat{\epsilon} \neq 0$, respectively) in Table 4. In the top line of the table, we impose $\hat{\epsilon} = 0$ and fit the remaining two parameters $\{\hat{g}_X, \theta_{sb}\}$ to show the fit of the original kinetically unmixed $B_3 - L_2$ model. In the bottom line of the table, we show the three-parameter $\{\hat{\epsilon}, \hat{g}_X, \theta_{sb}\}$ fit to the malaphoric $B_3 - L_2$ model, i.e. including kinetic mixing. We see from the table that kinetic mixing improves the fit⁶ by 7.3 units of χ^2 at the expense of introducing one additional free parameter $\hat{\epsilon}$. We see from the table that the improvement over $\hat{\epsilon} = 0$ is mainly due to improving the fit to flavour data in the ‘quarks’ and to the ‘LFU’ categories of observables. 95% constraints upon the $\hat{\epsilon} = 0$ $B_3 - L_2$ model from flavour measurements (albeit with previous lepton flavour unification data which favoured larger new physics effects) were presented in Refs. [23]. The malaphoric

⁶The p –value of such a change is .06.

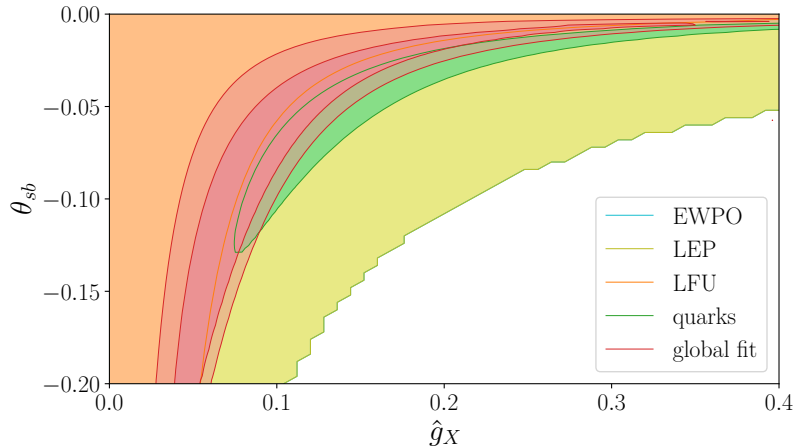


Figure 2. Parameter space of the unmixed $B_3 - L_2$ Z' model. White regions of parameter space are where `flavio2.6.1` could not constrain the CKM matrix elements to have an absolute value less than or equal to 1; in practice such regions are highly excluded by flavour measurements. The coloured region shows the 68% CL allowed region for each set of observable (as shown by reference to the legend). The global fit region is shown in red and shows both the 68% CL and the 95% CL. There is no region in the parameter space shown where the EWPO data provide a bad fit and so there is no EWPO contour shown.

$B_3 - L_2$ model shown in the bottom line has a $\Delta\chi^2$ of 40.1 in comparison to the SM. This is significant: the p -value of such a change, with 3 degrees of freedom (the effective number of free parameters) is $1. \times 10^{-8}$, indicating that the change is very unlikely to be due solely to random fluctuations of the measurements.

In Fig. 2, we show the fit to the $B_3 - L_2$ model for $\hat{\epsilon} = 0$, i.e. neglecting kinetic mixing. We see from the figure that the fit is not perfect because the preferred region of the ‘quarks’ category of observable does not overlap with the preferred region of the ‘LFU’ observables at the 68% confidence level (CL).

We show how this is improved by displaying the parameter space of the *malaphoric* $B_3 - L_2$ model in Fig. 3. We see from the plot that a parameter region exists which is preferred by the B -hadron decay data (‘quarks’) as well as LFU observables whilst simultaneously being compatible with LEP2 di-lepton production and measurements of EWPOs.

We display some observables of interest for the best-fit point of the malaphoric Z' model in Fig. 4. We see that many observables are fit better by the malaphoric $B_3 - L_2$ model than the SM, but a few (notably ΔM_s and $R_{K^{(*)}}(1.1, 6)$) have a somewhat worse fit in the malaphoric $B_3 - L_2$ model. M_W at the best-fit point is only marginally improved with respect to the SM value, which is some 2σ off the measurement. Many of the branching ratios in various bins of di-muon invariant mass squared are also better fit in the malaphoric $B_3 - L_2$ model. We note that in the malaphoric $B_3 - L_2$ model, several observables, although improved upon compared to the SM, are still not fit perfectly. This is reflected in the p -value of the

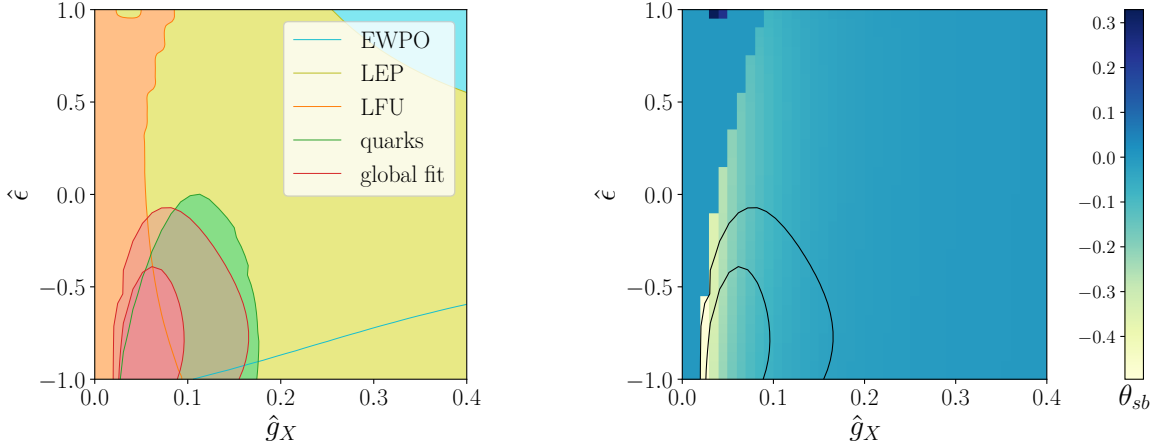


Figure 3. Parameter space of the malaphoric $B_3 - L_2$ Z' model, where θ_{sb} has been profiled over. In the left-hand plot, the coloured region shows the 68% CL allowed region for each set of observable (as shown by reference to the legend). The global fit region is shown in red and shows both the 68% CL and the 95% CL. In the right-hand plot, we show the best-fit value of θ_{sb} across the parameter plane.

model, which comes out to be⁷ .01.

We shall now try to gain some approximate qualitative analytic understanding of some of the results, neglecting the renormalisation effects (which were taken into account in our numerical results). It is known [32, 33] that in weak effective theory (WET) language, the fit improvements to $b \rightarrow s\ell^+\ell^-$ data come dominantly from assuming BSM contributions to $C_{9(\mu)}$, $C_{10(\mu)}$, $C_{9(e)}$ and $C_{10(e)}$, where we write the dimension-6 WET interaction Lagrangian as

$$\mathcal{L}_{WET} = \frac{4G_F}{\sqrt{2}} \sum_i (C_i^{\text{SM}} + C_i) \mathcal{O}_i + H.c., \quad (4.2)$$

where G_F is the Fermi constant, C_i are dimension-6 BSM Wilson coefficients and of particular interest are the operators

$$\begin{aligned} \mathcal{O}_{9(\mu)} &:= \frac{e^2}{16\pi^2} (\bar{s}\gamma_\alpha P_L b)(\bar{\mu}\gamma^\alpha \mu), \\ \mathcal{O}_{10(\mu)} &:= \frac{e^2}{16\pi^2} (\bar{s}\gamma_\alpha P_L b)(\bar{\mu}\gamma^\alpha \gamma_5 \mu), \end{aligned} \quad (4.3)$$

where e is the electromagnetic gauge coupling, P_L is the spinorial left-handed projection operator $(1 - \gamma_5)/2$, μ is the muon field, b the bottom quark field and s the strange quark field.

⁷The p -value of the $\hat{\epsilon} = 0$ $B_3 - L_2$ model is .006.

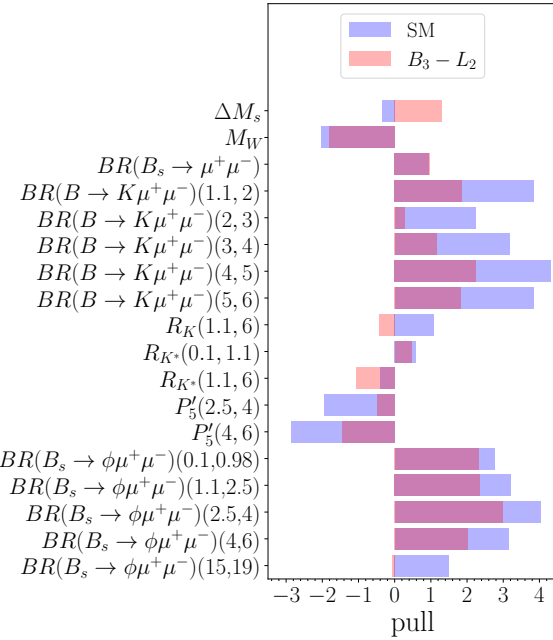


Figure 4. Some observables of interest from `flavio2.6.1` for the malaphoric $B_3 - L_2$ model at its best fit point (listed in Table 4). The ‘pull’ is defined as theory prediction minus the experimental central value, all divided by uncertainty neglecting any correlations. Where an observable has parenthesis with two numerical values enclosed, it is for that particular bin in di-muon invariant mass squared in units of GeV^2 .

$\mathcal{O}_{9(e)}$ and $\mathcal{O}_{10(e)}$ are obtained by replacing the muon field μ by the electron field e everywhere in (4.3). The same four operators have a version with a prime, where the projection operator is switched from $P_L \rightarrow P_R := (1 + \gamma_5)/2$. In the malaphoric $B_3 - L_2$ model presented here, the matching [34] between the SMEFT and the WET implies that the aforementioned primed operators all vanish and moreover that

$$\begin{aligned}
 C_{9(\mu)}/K &= -\frac{g_X \sin 2\theta_{sb}}{M_X^2} [3g_X + g'\epsilon(s_W^2 - 1)], \\
 C_{9(e)}/K &= -\frac{g_X \sin 2\theta_{sb}}{M_X^2} g'\epsilon(s_W^2 - 1), \\
 C_{10(\mu)} &= C_{10(e)} = 0,
 \end{aligned} \tag{4.4}$$

where $s_W := \sin \theta_W$, θ_W is the Weinberg angle and $K := 2\sqrt{2}\pi^2/(e^2 G_F)$; see Appendix A for more details. We see from (4.4) that, to obtain LFU in $b \rightarrow s\ell^+\ell^-$ transitions i.e. $C_{9(\mu)} = C_{9(e)}$, one would require $g_X = 0$. However, Ref. [18] showed that having $C_{9(e)} = C_{9(\mu)}/2$ is a close-to-optimal fit (to data similar to those taken here) along a particular line of models. Ref. [18] also showed, though, that having $C_{9(e)} = C_{9(\mu)}$ or even $C_{9(e)} = 0$ is within the 95% CL, providing statistical wiggle room.

The branching ratio of $B_s \rightarrow \mu^+ \mu^-$ can receive a BSM contribution to its SM prediction $BR(B_s \rightarrow \mu^+ \mu^-)^{\text{SM}}$ in Z' models with zero primed operators [23]:

$$BR(B_s \rightarrow \mu^+ \mu^-) = \left| 1 + \frac{C_{10}(\mu)}{C_{10}^{\text{SM}}} \right|^2 BR(B_s \rightarrow \mu^+ \mu^-)^{\text{SM}}. \quad (4.5)$$

The fact that $C_{10}(\mu) = 0$ in the malaphoric $B_3 - L_2$ model despite mixing with the hypercharge gauge boson which has chiral interactions, constrains the $B_s \rightarrow \mu^+ \mu^-$ branching ratio to be identical to the SM prediction, within our approximation. This is borne out at the best-fit point, as Fig. 4 shows.

The $B_s - \bar{B}_s$ mixing observable ΔM_s , receives a correction in the malaphoric $B_3 - L_2$ model identical to that of the $\hat{\epsilon} = 0$ limit, namely [23]

$$\frac{\Delta M_s}{\Delta M_s^{\text{SM}}} = \left| 1 + \frac{\eta(M_X) g_X^2 \sin^2 2\theta_{sb}}{8R_{\text{SM}}^{\text{loop}} M_X^2} \frac{\sqrt{2}}{4G_F (V_{tb} V_{ts}^*)^2} \right|, \quad (4.6)$$

where $R_{\text{SM}}^{\text{loop}} = 1.3397 \times 10^{-3}$ and $\eta(M_X)$ parameterise renormalisation effects: $\eta(M_X)$ varies between 0.79 and 0.74 when M_X ranges between 1 and 10 TeV [35]. The SM prediction of ΔM_s is in good agreement with the measurement, whereas (4.6) shows that one acquires a positive contribution from the malaphoric $B_3 - L_2$ model, as shown in Fig 4. Such a contribution then has a preference for smaller values of $|\hat{g}_X \sin 2\theta_{sb}|$ in the fit.

The prediction of M_W receives a positive contribution from the changes to $C_{\varphi \square}$ and $C_{\varphi D}$ in (2.29) and (2.30). As Fig. 4 shows, a positive contribution is preferred by the current measurements but in practice, for the best-fit point at least, such a change is rather small.

5 Summary

We have calculated the dimension-6 SMEFT Wilson coefficients resulting from integrating out a kinetically-mixed TeV-scale Z' field resulting from a spontaneously broken $U(1)_X$ gauge symmetry. Such Wilson coefficients were recently calculated⁸ for a generic heavy Z' model including kinetic mixing in Ref. [24]. After we found a few sign errors in the dimension-6 coefficients of the original *pre-erratum* version of that pioneering paper, the authors of Ref. [24] have graciously confirmed that they agree with our expressions, which are tabulated in (2.8)-(2.30).

We apply the SMEFT Wilson coefficients mentioned above to the case of a Z' model (the $B_3 - L_2$ model) that was originally designed to fit $b \rightarrow s\ell^+\ell^-$ data, which are at odds with their SM predictions. To our knowledge, this is the first time that kinetic mixing has been taken into account in fits to $b \rightarrow s\ell^+\ell^-$ data. When kinetic mixing is small, this $B_3 - L_2$ model contains rather too much lepton flavour universality violation and did not fit more recent analyses of R_K and R_{K^*} by the LHCb Collaboration well. We have shown that

⁸Ref. [24] also calculates the dimension-8 coefficients, finding that dimension-8 coefficients are generically too small to affect the phenomenology much. We neglect them here.

including a sizeable kinetic mixing between the new $U(1)$ gauge boson and the hypercharge gauge boson provides an improved fit to $b \rightarrow s\ell^+\ell^-$ measurements. Such a fit comes about partly because the kinetic mixing contribution respects lepton flavour universality. Various papers [32, 33, 36, 37] have pointed out that a LFU contribution to the WET Wilson coefficient C_9 as well as an enhanced contribution to $C_{9(\mu)}$ provides an improved fit. We see from the pieces proportional to ϵ in (4.4) how the kinetic mixing in the malaphoric $B_3 - L_2$ model provides such a LFU contribution. In addition, we see in (4.4) that, despite the fact that the Z' contains a component of the hypercharge gauge boson (which couples chirally), the resulting propagating eigenstate couples to left-handed leptons with the same strength that it couples to right-handed leptons, to a good approximation.

Other approaches to explain neutral current $b \rightarrow s\ell^+\ell^-$ anomalies after the updated R_K and R_{K^*} analyses have been taken. For example, in Ref. [18] a model which had $U(1)_X$ charge assignments corresponding to $X := 3B_3 - L_e - 2L_\mu$, where L_e is first-family lepton number, was found to fit the flavour measurements including the current ones for R_K and R_{K^*} reasonably well as a whole even neglecting kinetic mixing. The assignment $X := 3B_3 - L$ where L is lepton number, has also been studied [18, 36]. Some authors have introduced several new $U(1)$ gauge bosons with family-dependent hypercharge-like assignments [38, 39]; these can have various advantages from the point of view of motivating observed hierarchies in fermion masses.

Returning to the unmixed $B_3 - L_2$ model, with the assumptions about fermion mixing detailed in § 3, the Z' does couples only very weakly to first generation quarks. Direct search bounds coming from non-observation of a di-lepton bump at the LHC collider are then rather weak because the production cross-section is doubly suppressed by bottom quark parton distribution functions, since $b\bar{b} \rightarrow Z'$ is the dominant production mode [40]. When kinetic mixing is introduced, this is no longer the case and it is likely that the direct search bounds will become stronger because the malaphoric $B_3 - L_2$ predicts a family universal component to the couplings to up and down quarks. However, since direct searches are beyond the scope of the present paper, we shall burn that bridge when we come to it.

Acknowledgements

This work was partially supported by STFC HEP Consolidated grants ST/T000694/1 and ST/X000664/1. We thank the Cambridge Pheno Working Group and P. Stangl for discussions and S. Dawson, M. Forslund and M. Schnubel for helpful comparisons of the dimension-6 SMEFT coefficients. We thank E. Loisa for comments on the manuscript. BCA thanks CERN for hospitality extended while part of this work was undertaken.

A WET Wilson Coefficients in the $B_3 - L_2$ model

The tree-level SMEFT to WET coefficient matching formulae are known [34] (we take C_{ledq}^{2223} and C_{ledq}^{2232} to vanish, as results from integrating out a Z'):

$$\begin{aligned}
C_{9(\mu)}/K &= C_{qe}^{2322} + (C_{lq}^{(1)})^{2223} + (C_{lq}^{(3)})^{2223} - (1 - 4s_W^2)[(C_{\varphi q}^{(1)})^{23} + (C_{\varphi q}^{(3)})^{23}], \\
C_{10(\mu)}/K &= C_{qe}^{2322} - (C_{lq}^{(1)})^{2223} - (C_{lq}^{(3)})^{2223} + (C_{\varphi q}^{(1)})^{23} + (C_{\varphi q}^{(3)})^{23}, \\
C_{9(e)}/K &= C_{qe}^{2311} + (C_{lq}^{(1)})^{1123} + (C_{lq}^{(3)})^{1123} - (1 - 4s_W^2)[(C_{\varphi q}^{(1)})^{23} + (C_{\varphi q}^{(3)})^{23}], \\
C_{10(e)}/K &= C_{qe}^{2311} - (C_{lq}^{(1)})^{1123} - (C_{lq}^{(3)})^{1123} + (C_{\varphi q}^{(1)})^{23} + (C_{\varphi q}^{(3)})^{23}, \\
C'_{9(\mu)}/K &= C_{ed}^{2223} + C_{ld}^{2223} - (1 - 4s_W^2)C_{\varphi d}^{23}, \\
C'_{10(\mu)}/K &= C_{ed}^{2223} - C_{ld}^{2223} + C_{\varphi d}^{23}, \\
C'_{9(e)}/K &= C_{ed}^{1123} + C_{ld}^{1123} - (1 - 4s_W^2)C_{\varphi d}^{23}, \\
C'_{10(e)}/K &= C_{ed}^{1123} - C_{ld}^{1123} + C_{\varphi d}^{23}.
\end{aligned} \tag{A.1}$$

Since we have set V_{d_R} to be the 3 by 3 identity matrix, $(C_{\varphi d})_{23} = 0$ in the $B_3 - L_2$ model. Thus, note that all of the SMEFT coefficients on the right-hand sides of $C'_{9/10(e/\mu)}$ are zero at tree-level. From (2.20) and (2.21) and the charges in Table 3, we have

$$\begin{aligned}
(C_{lq}^{(1)})^{2223} &= -\frac{1}{M_X^2}(-3g_X + g'\epsilon/2)\Xi_{23}, \\
(C_{lq}^{(1)})^{1123} &= -\frac{1}{2M_X^2}g'\epsilon\Xi_{23}, \\
C_{qe}^{2322} &= -\frac{1}{M_X^2}(-3g_X + g'\epsilon)\Xi_{23}, \\
C_{qe}^{2311} &= -\frac{1}{M_X^2}g'\epsilon\Xi_{23}
\end{aligned} \tag{A.2}$$

The only other relevant non-zero dimension-6 SMEFT coefficient given by the malaphoric $B_3 - L_2$ model is

$$(C_{\varphi q}^{(1)})^{23} = \frac{1}{2M_X^2}g'\epsilon\Xi_{23}, \tag{A.3}$$

as can be seen from (2.24). Substituting (A.2) and (A.3) into (A.1), we arrive at (4.4).

B Integrating out the X_μ field

To integrate out the X_μ field we use the path integral formalism. The part of the generating functional relevant for our discussion reads

$$Z[J] = \int [dX_\mu] \exp \left[i \int d^4x \left(-\frac{1}{4}X_{\mu\nu}X^{\mu\nu} + \frac{1}{2}M_X^2X_\mu X^\mu - \frac{\epsilon}{2}B_{\mu\nu}X^{\mu\nu} - X_\mu J^\mu \right) \right], \tag{B.1}$$

with the notation introduced in the §2 and where $[dX_\mu]$ denotes the integration over all the paths with the correct boundary conditions. The penultimate term in the equation above can be rewritten as

$$X_{\mu\nu}B^{\mu\nu} \equiv (\partial_\mu X_\nu - \partial_\nu X_\mu)B^{\mu\nu} = -2(\partial_\nu X_\mu)B^{\mu\nu} \implies 2X_\mu(\partial_\nu B^{\mu\nu}), \quad (\text{B.2})$$

where the last equality is derived by integration by parts of the action. We cast (B.1) in the form

$$\begin{aligned} Z[J] &= \int [dX_\mu] \exp \left[\frac{i}{2} \int d^4x d^4y X_\mu(x) \mathcal{K}^{\mu\nu}(x, y) X_\nu(y) - i \int d^4x X_\mu \hat{J}^\mu \right] \\ &= \int [dX_\mu] \exp \left[\frac{i}{2} \int d^4x d^4y \right. \\ &\quad \left(X_\mu(x) + \int d^4u \hat{J}^\alpha(u) \Delta_{\alpha\mu}(u, x) \right) \mathcal{K}^{\mu\nu}(x, y) \left(X_\nu(y) + \int d^4v \Delta_{\nu\beta}(y, v) \hat{J}^\beta(v) \right) \\ &\quad \left. - \frac{i}{2} \int d^4x d^4y \hat{J}^\mu(x) \Delta_{\mu\nu}(x, y) \hat{J}^\nu(y) \right], \end{aligned}$$

where

$$\begin{aligned} \mathcal{K}^{\mu\nu}(x, y) &= \delta^{(4)}(x - y) (g^{\mu\nu}(\partial^2 + M_X^2) - \partial^\mu \partial^\nu), \\ \hat{J}^\mu &= J^\mu + \epsilon(\partial_\nu B^{\mu\nu}), \\ \int d^4y \mathcal{K}_{\mu\nu}(x, y) \Delta^{\nu\lambda}(y, z) &= g_\mu^\lambda \delta^{(4)}(x - z), \\ \Delta_{\mu\nu}(x, y) &= \int \frac{d^4k}{(2\pi)^4} \Delta_{\mu\nu}(k) e^{-k(x-y)}, \\ \Delta_{\mu\nu}(k) &= -\frac{1}{k^2 - M_X^2} \left(g_{\mu\nu} - \frac{k_\mu k_\nu}{M_X^2} \right). \end{aligned} \quad (\text{B.3})$$

Performing the replacement $X \mapsto X - \Delta J$, the functional integral over dX can be easily performed (it gives an infinite constant that can be ignored):

$$\begin{aligned} Z[J] &= \exp \left[-\frac{i}{2} \int d^4x d^4y \hat{J}^\mu(x) \Delta_{\mu\nu}(x, y) \hat{J}^\nu(y) \right] \\ &\quad \times \int [dX_\mu] \exp \left[\frac{i}{2} \int d^4x d^4y X_\mu(x) \mathcal{K}^{\mu\nu}(x, y) X_\nu(y) \right] \\ &\propto \exp \left[-\frac{i}{2} \int d^4x d^4y \hat{J}^\mu(x) \Delta_{\mu\nu}(x, y) \hat{J}^\nu(y) \right]. \end{aligned} \quad (\text{B.4})$$

Finally, expanding in the limit $M_X^2 \gg k^2$, we obtain

$$\Delta_{\mu\nu}(x, y) \simeq \frac{g_{\mu\nu}}{M_X^2} \delta^{(4)}(x - y), \quad (\text{B.5})$$

and hence

$$\mathcal{L}_6 = -\frac{1}{2M_X^2} \hat{J}^\mu \hat{J}_\nu \equiv -\frac{1}{2M_X^2} J_\mu J^\mu - \frac{\epsilon}{M_X^2} (\partial_\nu B^{\mu\nu}) J_\mu - \frac{\epsilon^2}{2M_X^2} (\partial_\nu B^{\mu\nu})(\partial^\rho B_{\mu\rho}), \quad (\text{B.6})$$

which coincides with the first line in Eq. (9) of Ref. [24]. The same result can be achieved using the equations of motion for the X_μ field:

$$\partial_\nu X^{\mu\nu} = -J^\mu - \epsilon \partial_\nu B^{\mu\nu} + M_X^2 X^\mu, \quad (\text{B.7})$$

$$\implies X^\mu = \frac{1}{M_X^2} (\partial_\nu X^{\mu\nu} + J^\mu + \epsilon \partial_\nu B^{\mu\nu}). \quad (\text{B.8})$$

Substituting this expression into (2.1) gives (2.5).

References

- [1] N. Gubernari, M. Reboud, D. van Dyk and J. Virto, *Improved theory predictions and global analysis of exclusive $b \rightarrow s\mu^+\mu^-$ processes*, *JHEP* **09** (2022) 133 [[2206.03797](#)].
- [2] **HPQCD** Collaboration, W. G. Parrott, C. Bouchard and C. T. H. Davies, *Standard Model predictions for $B \rightarrow K\ell+\ell-$, $B \rightarrow K\ell 1\ell 2+$ and $B \rightarrow K\nu\bar{\nu}$ using form factors from $Nf=2+1+1$ lattice QCD*, *Phys. Rev. D* **107** (2023), no. 1 014511 [[2207.13371](#)]. [Erratum: *Phys. Rev. D* 107, 119903 (2023)].
- [3] **LHCb** Collaboration, R. Aaij *et. al.*, *Measurement of CP -Averaged Observables in the $B^0 \rightarrow K^{*0}\mu^+\mu^-$ Decay*, *Phys. Rev. Lett.* **125** (2020), no. 1 011802 [[2003.04831](#)].
- [4] **ATLAS** Collaboration, M. Aaboud *et. al.*, *Angular analysis of $B_d^0 \rightarrow K^*\mu^+\mu^-$ decays in pp collisions at $\sqrt{s} = 8$ TeV with the ATLAS detector*, *JHEP* **10** (2018) 047 [[1805.04000](#)].
- [5] **CMS** Collaboration, A. M. Sirunyan *et. al.*, *Measurement of angular parameters from the decay $B^0 \rightarrow K^{*0}\mu^+\mu^-$ in proton-proton collisions at $\sqrt{s} = 8$ TeV*, *Phys. Lett. B* **781** (2018) 517–541 [[1710.02846](#)].
- [6] **LHCb** Collaboration, R. Aaij *et. al.*, *Measurements of the S-wave fraction in $B^0 \rightarrow K^+\pi^-\mu^+\mu^-$ decays and the $B^0 \rightarrow K^*(892)^0\mu^+\mu^-$ differential branching fraction*, *JHEP* **11** (2016) 047 [[1606.04731](#)]. [Erratum: *JHEP* 04, 142 (2017)].
- [7] **LHCb** Collaboration, R. Aaij *et. al.*, *Differential branching fractions and isospin asymmetries of $B \rightarrow K^{(*)}\mu^+\mu^-$ decays*, *JHEP* **06** (2014) 133 [[1403.8044](#)].
- [8] **CMS** Collaboration, A. Hayrapetyan *et. al.*, *Test of lepton flavor universality in $B^\pm \rightarrow K^\pm\mu^+\mu^-$ and $B^\pm \rightarrow K^\pm e^+e^-$ decays in proton-proton collisions at $\sqrt{s} = 13$ TeV*, *Rept. Prog. Phys.* **87** (2024), no. 7 077802 [[2401.07090](#)].
- [9] **LHCb** Collaboration, R. Aaij *et. al.*, *Branching Fraction Measurements of the Rare $B_s^0 \rightarrow \phi\mu^+\mu^-$ and $B_s^0 \rightarrow f_2'(1525)\mu^+\mu^-$ Decays*, *Phys. Rev. Lett.* **127** (2021), no. 15 151801 [[2105.14007](#)].
- [10] S. Mutke, M. Hoferichter and B. Kubis, *Anomalous thresholds in $B \rightarrow (P, V)\gamma^*$ form factors*, *JHEP* **07** (2024) 276 [[2406.14608](#)].
- [11] P. Ball, G. W. Jones and R. Zwicky, *$B \rightarrow V\gamma$ beyond QCD factorisation*, *Phys. Rev. D* **75** (2007) 054004 [[hep-ph/0612081](#)].
- [12] G. Isidori, Z. Polonsky and A. Tinari, *An explicit estimate of charm rescattering in $B^0 \rightarrow K^0\bar{\ell}\ell$* , [2405.17551](#).

[13] N. Gubernari, D. van Dyk and J. Virto, *Non-local matrix elements in $B_{(s)} \rightarrow \{K^{(*)}, \phi\} \ell^+ \ell^-$* , *JHEP* **02** (2021) 088 [[2011.09813](#)].

[14] **LHCb** Collaboration, R. Aaij *et. al.*, *Test of lepton universality in $b \rightarrow s \ell^+ \ell^-$ decays*, [2212.09152](#).

[15] J. Aebischer, J. Kumar and D. M. Straub, *Wilson: a Python package for the running and matching of Wilson coefficients above and below the electroweak scale*, *Eur. Phys. J. C* **78** (2018), no. 12 1026 [[1804.05033](#)].

[16] J. Aebischer, J. Kumar, P. Stangl and D. M. Straub, *A Global Likelihood for Precision Constraints and Flavour Anomalies*, *Eur. Phys. J. C* **79** (2019), no. 6 509 [[1810.07698](#)].

[17] D. M. Straub, *flavio: a Python package for flavour and precision phenomenology in the Standard Model and beyond*, [1810.08132](#).

[18] B. Allanach and A. Mullin, *Plan B: new Z' models for $b \rightarrow s \ell^+ \ell^-$ anomalies*, *JHEP* **09** (2023) 173 [[2306.08669](#)].

[19] **LHCb** Collaboration, R. Aaij *et. al.*, *Test of lepton universality in beauty-quark decays*, *Nature Phys.* **18** (2022), no. 3 277–282 [[2103.11769](#)]. [Addendum: *Nature Phys.* 19, (2023)].

[20] C. Bonilla, T. Modak, R. Srivastava and J. W. F. Valle, *$U(1)_{B_3-3L_\mu}$ gauge symmetry as a simple description of $b \rightarrow s$ anomalies*, *Phys. Rev. D* **98** (2018), no. 9 095002 [[1705.00915](#)].

[21] R. Alonso, P. Cox, C. Han and T. T. Yanagida, *Flavoured $B - L$ local symmetry and anomalous rare B decays*, *Phys. Lett. B* **774** (2017) 643–648 [[1705.03858](#)].

[22] B. C. Allanach, *$U(1)_{B_3-L_2}$ explanation of the neutral current B -anomalies*, *Eur. Phys. J. C* **81** (2021), no. 1 56 [[2009.02197](#)]. [Erratum: *Eur.Phys.J.C* 81, 321 (2021)].

[23] B. Allanach and J. Davighi, *The Rumble in the Meson: a leptoquark versus a Z' to fit $b \rightarrow s \mu^+ \mu^-$ anomalies including 2022 LHCb $R_{K^{(*)}}$ measurements*, *JHEP* **04** (2023) 033 [[2211.11766](#)].

[24] S. Dawson, M. Forsslund and M. Schnubel, *SMEFT Matching to Z' Models at Dimension-8*, [2404.01375](#).

[25] K. S. Babu, C. F. Kolda and J. March-Russell, *Implications of generalized Z - Z -prime mixing*, *Phys. Rev. D* **57** (1998) 6788–6792 [[hep-ph/9710441](#)].

[26] H.-C. Cheng, X.-H. Jiang, L. Li and E. Salvioni, *Dark showers from Z -dark Z' mixing*, *JHEP* **04** (2024) 081 [[2401.08785](#)].

[27] B. Grzadkowski, M. Iskrzynski, M. Misiak and J. Rosiek, *Dimension-Six Terms in the Standard Model Lagrangian*, *JHEP* **10** (2010) 085 [[1008.4884](#)].

[28] **Particle Data Group** Collaboration, R. L. Workman *et. al.*, *Review of Particle Physics*, *PTEP* **2022** (2022) 083C01.

[29] A. Celis, J. Fuentes-Martin, A. Vicente and J. Virto, *DsixTools: The Standard Model Effective Field Theory Toolkit*, *Eur. Phys. J. C* **77** (2017), no. 6 405 [[1704.04504](#)].

[30] J. Aebischer *et. al.*, *WCxf: an exchange format for Wilson coefficients beyond the Standard Model*, *Comput. Phys. Commun.* **232** (2018) 71–83 [[1712.05298](#)].

- [31] **Particle Data Group** Collaboration, S. Navas *et. al.*, *Review of particle physics*, *Phys. Rev. D* **110** (2024), no. 3 030001.
- [32] M. Algueró, A. Biswas, B. Capdevila, S. Descotes-Genon, J. Matias and M. Novoa-Brunet, *To (b)e or not to (b)e: no electrons at LHCb*, *Eur. Phys. J. C* **83** (2023), no. 7 648 [[2304.07330](#)].
- [33] T. Hurth, F. Mahmoudi and S. Neshatpour, *B anomalies in the post $R_{K^{(*)}}$ era*, *Phys. Rev. D* **108** (2023), no. 11 115037 [[2310.05585](#)].
- [34] J. Aebischer, A. Crivellin, M. Fael and C. Greub, *Matching of gauge invariant dimension-six operators for $b \rightarrow s$ and $b \rightarrow c$ transitions*, *JHEP* **05** (2016) 037 [[1512.02830](#)].
- [35] L. Di Luzio, M. Kirk and A. Lenz, *Updated B_s -mixing constraints on new physics models for $b \rightarrow s\ell^+\ell^-$ anomalies*, *Phys. Rev. D* **97** (2018), no. 9 095035 [[1712.06572](#)].
- [36] A. Greljo, J. Salko, A. Smolkovič and P. Stangl, *Rare b decays meet high-mass Drell-Yan*, *JHEP* **05** (2023) 087 [[2212.10497](#)].
- [37] M. Ciuchini, M. Fedele, E. Franco, A. Paul, L. Silvestrini and M. Valli, *Constraints on lepton universality violation from rare B decays*, *Phys. Rev. D* **107** (2023), no. 5 055036 [[2212.10516](#)].
- [38] J. Davighi and B. A. Stefanek, *Deconstructed hypercharge: a natural model of flavour*, *JHEP* **11** (2023) 100 [[2305.16280](#)].
- [39] M. Fernández Navarro, S. F. King and A. Vicente, *Minimal complete tri-hypercharge theories of flavour*, *JHEP* **07** (2024) 147 [[2404.12442](#)].
- [40] B. C. Allanach, J. M. Butterworth and T. Corbett, *Large hadron collider constraints on some simple Z' models for $b \rightarrow s\mu^+\mu^-$ anomalies*, *Eur. Phys. J. C* **81** (2021), no. 12 1126 [[2110.13518](#)].